Cite this article
Moghadam SH, Ashofteh PS and Loáiciga HA
Use of surface water and groundwater under climate change: Khorramabad basin, Iran.
Proceedings of the Institution of Civil Engineers – Water Management,
https://doi.org/10.1680/jwama.19.00011

Research Article
Paper 1900011
Received 25/02/2019;
Accepted 15/01/2021

Keywords: climate change/groundwater/water supply

Water Management

ice Publishing

Use of surface water and groundwater under climate change: Khorramabad basin, Iran

Seyedeh Hadis Moghadam BSc
Postgraduate student, Department of Civil Engineering, University of Qom, Qom, Iran

Parisa-Sadat Ashofteh PhD
Assistant Professor, Department of Civil Engineering, University of Qom, Qom, Iran (corresponding author: ps.ashofteh@qom.ac.ir)

Hugo A. Loáiciga PhD
Professor, Department of Geography, University of California, Santa Barbara, CA, USA

The impacts of climate change on the conjunctive use of surface water and groundwater resources of the Khorramabad basin were evaluated. Monthly temperature and rainfall modelled using HadCM3 and CGCM2 under greenhouse gas emissions scenarios (GHGESs) A2 and B2 were downscaled to baseline (1971–2000) and future periods (2040–2069 and 2070–2099). Simulations were performed for four climate change scenarios (CCSs) (A2-2040–2069, A2-2070–2099, B2-2040–2069 and B2-2070–2099). The projections indicated an increase in temperature and a decrease in rainfall. Future surface water resources were simulated using IHACRES. The results indicated that average annual runoff under GHGESs A2 and B2 would decrease by, respectively, 2.03% and 4.17% in 2040–2069 and by 6.64% and 8.94% in 2070–2099. Groundwater simulation was carried out using ModFlow. The results showed that under, the four CCSs, groundwater level would decline by 2.3%, 3.0%, 2.5% and 3.4%, respectively, relative to the baseline. Aquifer recharge under the four scenarios would decline by 1.43%, 5.71%, 2.86% and 7.14%, respectively. The results from IHACRES and ModFlow were employed to develop a conjunctive operation model with the Weap model. Several CCSs with various levels of future water demand were assessed using Weap. A 20% increase in water demand relative to the baseline, for instance, was projected to produce annual deficits in future agricultural water supply of 3.3, 5.08, 3.05 and 5.18 ($\times 10^6$ m^3), respectively, under the four CCSs.

1. Introduction

Climate change may adversely affect hydro-climatic parameters such as temperature, precipitation, surface water and groundwater (SWGW) flows (IPCC, 2007). In addition, populations and water use continue to increase. The possible worsening of freshwater scarcity and concomitant use of water calls for improved conjunctive use of SWGW resources.

Several studies concerning the conjunctive use of SWGW have been reported. Buras (1963) analysed the conjunctive use of a surface reservoir and a groundwater aquifer. Dynamic programming was applied to develop an optimal operating rule and an optimal policy was obtained as a steady-state solution. Employing a genetic algorithm (GA) and artificial neural network (ANN), Karamouz *et al.* (2004) developed a methodology for the conjunctive use of SWGW resources. Water supply, reduction of pumping costs and controlling groundwater table fluctuations were considered in the objective function of the model, which was applied to SWGW allocation in the southern part of Tehran, Iran. Karamouz *et al.* (2005) evaluated the conjunctive use of SWGW resources with an emphasis on water quality. Polluted surface waters were used in conjunction with groundwater for irrigation purposes in the southern part of Tehran. The results indicated the significance of an integrated approach to allocation of SWGW resources. Korkmaz *et al.* (2016) followed a deterministic approach to obtain a water-diversion function through the development of a numerical model for the city of Eskisehir, Turkey. The three criteria considered were ecosystem conservation, flood prevention and aquifer replenishment. The basin was modelled using ModFlow with GMS software. Transient simulations were performed over a period of 650 days covering low and high flows. The proposed function was found to be successful in satisfying all three criteria. Heydari *et al.* (2016) developed a multi-objective water allocation model for optimisation of the conjunctive use of SWGW resources in the Najaf Abad plain, Iran. The water resource allocation model was based on the simulation–optimisation modelling approach. An ANN (for groundwater level simulation) and genetic programming (for the prediction of total dissolved solids concentration) were coupled with a non-dominated sorting GA (NSGA-II). Li *et al.* (2016) established a conjunctive model to regulate SWGW allocations in an arid river basin in northwestern China. Their results showed that the current water resources were sufficient to meet the highest priority water needs (daily water supply, industry, ecological environment), but there was insufficient water to meet the needs of irrigated agriculture in its current form. Mani *et al.* (2016) developed a conjunctive-use model for the management of SWGW resources using mixed integer linear fractional programming. The objective of the conjunctive-use model was to maximise the ratio of groundwater usage to surface water usage through a water supply network to raise the groundwater level in the Sparta aquifer in the Ouachita, Lincoln and Union parishes of Louisiana, USA, while maximising groundwater pumping. Ashofteh *et al.* (2017) evaluated the Gharanghu multi-purpose reservoir system (east Azerbaijan, Iran). Simulation results using the water evaluation and planning (Weap) model were applied to

determine the efficiency indexes of the multi-purpose reservoir system under climate change projections. Safavi and Falsafioun (2017) applied a GA to two scenarios of deficit irrigation in search of optimal conjunctive use of SWGW resources in the Nekouabad irrigation district of the Zayandehrud basin, Iran.

Projections of future climate in Iran show reductions in future precipitation and runoff. This water scarcity will be compounded by population growth and concomitant increasing water use. In this context, the optimised conjunctive use of SWGW resources may be a viable adaption measure to adverse climate impacts for a growing population. Although various studies have been carried out on the conjunctive use of SWGW, most have not addressed the effect of climate change on conjunctive systems. For example, Safavi *et al.* (2009) reported a simulation–optimisation method for the conjunctive use of SWGW in west-central Iran (Najafabad plain), with the objective of minimising water shortages while meeting irrigation demands and the maximum capacity of surface irrigation systems. Tabari and Soltani (2012) developed a model for SWGW conjunctive-use management to maximise system reliability and minimise costs. For this purpose, the NSGA-II was applied, and the results were compared with the results of a sequential GA. Singh (2014) presented various methods for the conjunctive use of SWGW resources, and explained the advantages and disadvantages of each. Tabari (2015) applied combined fuzzy logic and a direct search optimisation technique to account for the uncertainty associated with parameters that affect fluctuations in groundwater level.

The aim of the work reported in this article was to evaluate the effect of climate change phenomena on the conjunctive use of SWGW systems. Using HadCM3 (Hadley Centre coupled model version 3) and CGCM2 (coupled general circulation model version 2), temperature and rainfall climate data were projected for a baseline period (1971–2000) and future periods (2040–2069 and 2070–2099) under the A2 and B2 greenhouse gas emissions scenarios (GHGESs). The surface water resources of Khorramabad basin, located in Lorestan province, Iran, were projected with the IHACRES (Identification of unit hydrographs and component flows from rainfall, evaporation, and streamflow) model under GHGESs A2 and B2 in the periods 2040–2069 and 2070–2099. The projected temperature, rainfall and surface water resources projected under GHGESs A2 and B2 were then employed to implement groundwater simulations using ModFlow. The status of SWGW resources was simulated with the Weap model, leading to monthly water allocations to meet municipal/industrial (M&I) and agricultural demands.

2. Methodology

The location of the study area is described before presentation of the GHGESs, climate scenarios, downscaling of atmosphere–ocean general circulation models (AOGCMs) outputs, selection of the best models for temperature and rainfall, rainfall–runoff simulation, groundwater level modelling with ModFlow, simulation of water resources allocation with the Weap model and analysis of results. A flowchart of the methodology is provided in Figure 1.

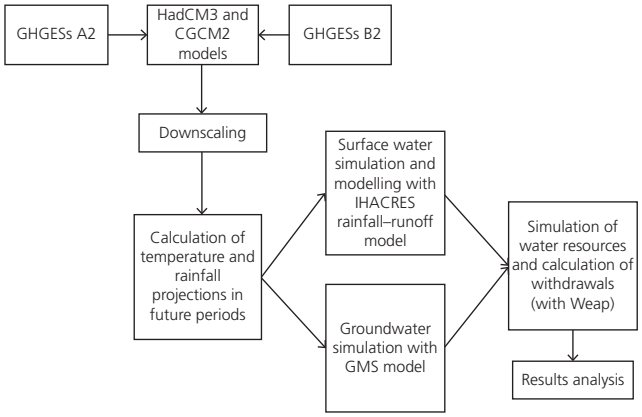

Figure 1. Flowchart of methodology

2.1 Geographic location of the case study

The study area of Khorramabad, Lorestan province, Iran is located between 47°55′E and 48°50′E longitude and 32°40′N and 34°20′N latitude. The main stream is the Khorramabad River. The area includes a main plain (central plain) and a few small scattered plains. The area of the case study is 2501.4 km^2, of which 8.5% is plains and 91.5% is at high elevation. Figure 2 shows the location of the study area. The Khorramabad stream flow is generated by rainfall and by spring flows and drainage from the highlands. Data from Cham-Anjir hydrometric station were used to estimate runoff volume and total annual reservoir inflow. The characteristics of the meteorological stations located within the study area are listed in Table 1. These hydrometric stations have data for the period 1971–2000, which was chosen as the baseline period in this work. The World Meteorological Organization (WMO) proposes using the baseline period 1961–1990 in climate change studies and carrying out comparisons with future period projections. However, based on the WMO recommendation, in cases where there are no data recorded at meteorological stations in the chosen study area, the period 1971–2000 is an alternative (IPCC, 2007; IPCC-TGCIA, 1999). Given the lack of data for 1961–1990, the period 1971–2000 was thus chosen as the baseline period. In addition, meteorological and hydrometric data were either incomplete or non-existent for the years 2000–2019. As also suggested by the WMO, the 30-year periods of 2040–2069 and 2070–2099 were considered as near and far future for climate change projections (IPCC, 2007).

2.2 Climate projections

Projections of future climate can be generated by AOGCMs (Lane *et al.*, 1999; Mitchell, 2003; Wilby and Harris, 2006).

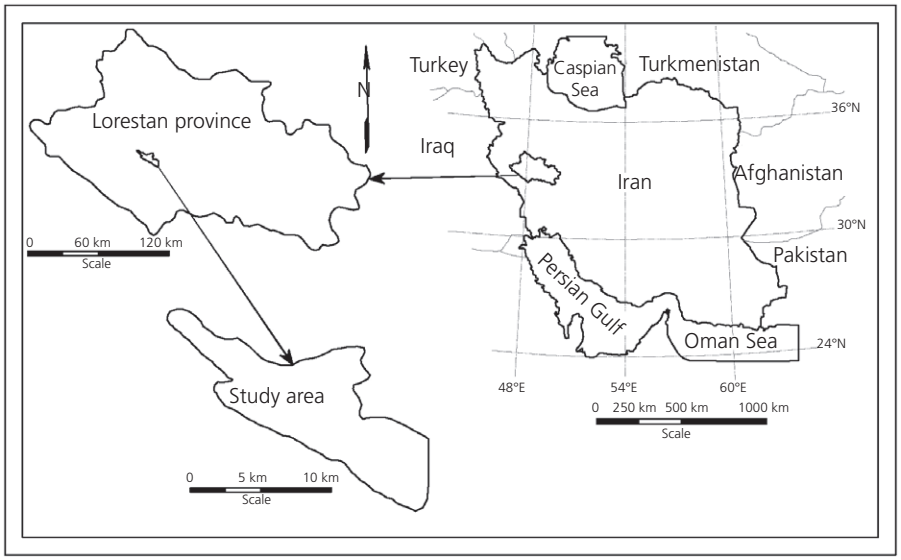

Figure 2. Location of study area in Lorestan province, Iran

Table 1. Characteristics of meteorological stations in the study basin

Station name	River basin	Longitude	Latitude	Elevation: m
Tang Valley	Ab-shotor	48–16°E	33–56°N	1730
Paul Keshkan	Khashkan	47–48°E	33–30°N	960
Kakarza	Harud	48–16°E	33–43°N	1550
Seyed Ali	Ab-shotor	48–13°E	33–48°N	1530
Sarkhab	Sezar	48–38°E	33–08°N	770
Tang-Siab	Ab-Siah	47–12°E	32–23°N	940
Cham-Anjir	Khorramabad	48–14°E	33–27°N	1166
Rahim-abad	Chalan Chulan	48–48°E	33–14°N	1490
Gol-Zard	Seimareh	47–21°E	33–11°N	680
Hulilan	Humian	47–15°E	33–44°N	1000
Poledokhtar	Payab Kashkan	47–43°E	33–10°N	700
Cham-chit	Goharrud	48–59°E	33–23°N	1290
Sepid-dasht	Sezar	48–53°E	33–47°N	970
Kuh-dasht	Madian-rud	47–37°E	33–32°N	970
Durud	Tireh	49–04°E	33–29°N	1450
Dehnu	Harude	48–46°E	33–30°N	1800
Afarineh	Cholhul	47–54°E	33–20°N	820
Afarineh	Kashkan	47–54°E	33–20°N	820
Khoramabad	Khoramabad	48–17°E	33–26°N	1147.8

This study relied on the outputs of HadCM3 for temperature and CGCM2 for rainfall (IPCC-TGCIA, 1999).

The path of future greenhouse gas (GHG) emissions is unknown; therefore, future GHG releases are projected under scenarios that envision a world whose characteristics depend on population growth, environmental protection and economic growth. There are four main GHGESs that serve as inputs to climatic models – B1, A2, A1 and B2 – and climate projections correspond to specific emissions scenarios. Specifically pertinent to this study are GHGESs B2 and A2.

- GHGES scenario A2 envisions a world in which countries operate independently and are self-reliant, the world's population is steadily increasing, economic development is region-oriented and there is high population growth and low dependence on rapid economic progress.
- GHGES scenario B2 is similar to A2, with the exception that it is environmentally friendly. In B2, the population increases steadily but its rate of growth is lower than that considered in A2;' it emphasises local solutions rather than global solutions to environmental stress and prescribes modest economic development.

Previous studies have shown that the approach of GHGES B2 may prevail in Iran and conforms well to possible future economic conditions and population studies in Iran. Therefore, B2 was considered in this study. On the other hand, because the largest amounts of GHGs would be produced in GHGES A2 (the most pessimistic scenario), A2 was also considered for analysis.

AOGCMs have noise in their predictions of climate variables. To overcome this problem it is customary to use a long-term average of their projections (Jones and Hulme, 1996). There are several methods used to downscale AOGCMs projections to basin-scale hydrologic models (Dettinger *et al*., 2004). The change-factor method for temporal downscaling (Loáiciga *et al*., 2000; Wilby and Harris, 2006) was implemented in this study.

2.3 Simulation of surface water resources

The IHACRES hydrologic model (Jakeman and Hornberger, 1993) was implemented for simulating the surface water resources of the Khorramabad basin. The IHACRES model is a rainfall–runoff integrated model that simulates river flows based on precipitation. It simulates river flows with the lowest values of input parameters (temperature and rainfall). IHACRES implements non-linear and linear modules to calculate precipitation losses and convert effective rainfall into runoff – the rainfall and temperature in each timestep produce effective precipitation using the non-linear module and the effective precipitation is converted to surface runoff in the same timestep with the linear module.

2.4 Simulation of groundwater resources

In this work, the ModFlow model was applied for groundwater simulations. The model inputs include recharge, observation wells, operation wells, aquifer boundaries, values of aquifer parameters, initial conditions, to name a few. Surface recharge consists of the percentage of rainfall penetration, the percentage of agricultural water reuse and the percentage of water reuse in drinking water and industrial sectors. Under climate change conditions, recharge is altered by changes in rainfall. The effect of climate change is accounted for by climate model projections corresponding to GHGESs A2 and B2.

In addition, GMS software was used for simulating groundwater. This software simulates groundwater processes, relying mainly on finite-difference and finite-element methods. GMS includes the groundwater models ModFlow, ModPath, the modular transport three-dimensional model simulator (MT3DMS), the reactive transport three-dimensional model (RT3D) and so on. One of the input parameters to GMS is the recharge rate, which generally depends on infiltration, evaporation, precipitation and soil type.

The study area was divided into polygons. These were used to define a numerical grid of the numerical groundwater model (ModFlow in this case) and recharge rates were applied to the polygons. Data obtained from the Lorestan Regional Water Corporation (LRWC, 2012) indicated that, in the study region, the average annual infiltration of agricultural water is 3.93×10^6 m^3, infiltration of M&I water is 3.96×10^6 m^3 and evaporation is 41.18×10^6 m^3. Cham-Anjir station gathers hydrometeorological data, and the data collected include those for the baseline period (1971–2000). Rainfall is constant within the study region. The soil type is generally alluvial in the central aquifer of the study area. Recharge rates were calculated as the sum of the percentage of the agricultural water use plus the percentage of effective precipitation plus the percentage of M&I water use. The effective precipitation was obtained by subtracting evaporation and losses from the rainfall. The recharge rate was input into the GMS conceptual model. Surface runoff is one of the variables calculated by GMS. The future values of rainfall and runoff change under climate change impacts, and these changes are taken into account in the GMS model. The effect of climate change is thus reflected in the hydroclimatic projections.

The effects of climate change on surface water resources were first investigated with the IHACRES model and the levels of future surface water change were projected under climatic scenarios. The effect of climate change on groundwater resources was calculated from climatic projections corresponding to GHGESs A2 and B2 that were input into the GMS software. The GMS model was calibrated by adjusting the hydraulic conductivity and other aquifer parameters until accurate predictions of measured groundwater levels and other aquifer variables were achieved. The runoff projected using IHACRES and the recharge determined by the GMS were then input into the Weap model. The reader is referred to coupled simulations reported by other authors (e.g. Alslevavni and Almohseen, 2017) for alternative approaches to cope with climate change impacts in hydroclimatic projections.

2.5 Simultaneous simulation of SWGW resources

The Weap model was used to assess the status of water resources. Weap is a comprehensive and widely used model for integrated water resources planning. The first application of Weap was carried out by Raskin *et al*. (1992) in the Aral basin, Central Asia. Based on the equations of water balance, Weap can be applied in urban and agricultural regions, independent basins or complex river systems. It applies to a wide range of situations such as analysing multi-sectoral water needs, water conservation, water rights and allocation priorities, simulations of SWGW, reservoir operation, hydropower generation, pollution routing, ecosystem needs, vulnerability assessment and project cost–benefit analysis. Weap implements a linear programming model to solve water allocation problems whose objective function is to maximise water supply according to the priorities of water supply and demand, mass balance and other constraints. All constraints

are defined for each simulation timestep and according to the water supply and demand priorities.

3. Results and discussion

3.1 Projection of future climate time series

HadCM3 and CGCM2 were applied to project climatic variables of temperature and rainfall during the baseline period. The models' predictive skill is measured by the coefficient of determination (R^2), the root mean square error (RMSE), the mean absolute error (MAE) and the Nash–Sutcliffe efficiency coefficient (NSE) (Ashofteh *et al.*, 2015). The results for GHGES A2 and B2 are listed in Tables 2 and 3, respectively. The higher the value of R^2 and the lower the errors, the better the model's predictive skill (performance). The results listed in Table 2 for GHGES A2 show that the performance of HadCM3 was acceptable. The CGCM2 model performed appropriately for the rainfall projections. For GHGES B2, according to Table 3, HadCM3 was suitable for the temperature projections and CGCM2 was better suited for the rainfall projections, as was the case for scenario A2. Overall, based on previous published works it may be concluded that, generally, general circulation models (GCMs) are more accurate with respect to temperature projections than precipitation projections. In addition, several studies have reported differing projections for temperature and precipitation by alternative climate models. Most previous studies show that temperature is generally rising, but this is not the case for precipitation (Asadi Vaighan *et al.*, 2017; Azadi *et al.*, 2019; Golfam *et al.*, 2019; Moghadam *et al.*, 2019). As already mentioned, one of the inputs of climate models is the pathway of future GHG emissions, which depends on economic, social and population growth, along with other variables. Several such pathways are commonly used in climate projections. Therefore, projections of climate variables are uncertain and this must be taken into account in future water resources management.

Climate change projections for temperature and rainfall in the study basin were calculated for the future periods. Climate change scenarios (CCSs) of temperature were calculated as the difference between the 30-year average temperature simulated by GCMs for each month of the future periods and the 30-year average temperature simulated by GCMs for each month of the baseline period, and adding the historical temperature to the difference in each month. CCSs of rainfall were calculated as the ratio of the 30-year average of rainfall simulated by GCMs for each month of future periods and the 30-year average rainfall simulated by GCMs for each month of the baseline period, and multiplying the ratio by the historic precipitation in each month (Loáiciga, 2000). The corresponding results are shown in Figures 3 and 4. It can be seen in Figure 3 that HadCM3 showed a rise in temperature for all months under both GHGESs and in both future periods. In the period 2040–2069 corresponding to GHGESs A2 and B2, temperature increases were projected to be 1–3.68°C and 1.52–1.62°C, respectively. In the period 2070–2099 for scenarios A2 and B2, the increases in temperature were predicted to be 2.69–7.29°C and 2.29–4.67°C, respectively. Comparison of the two future periods indicates that 2070–2099 is predicted to have a higher temperature than 2040–2069. In addition, scenario B2 provided a greater increase in temperature than scenario A2. In both periods and under both scenarios, the temperatures in the cold months of the year would be lower, while temperatures would be higher in the warm months.

Concerning rainfall, Figure 4 shows that CGCM2 in both scenarios and both future periods projected increases in some months and decreases in others. For the period 2040–2069, for GHGESs A2 and B2, the range of rainfall variation was

Table 2. Predictive skills of climatic models under GHGES A2

	Performance criterion							
	Temperature				Rainfall			
Model	R^2: %	RMSE: °C	MAE: °C	NSE	R^2: %	RMSE: mm	MAE: mm	NSE
HadCM3	94.3	3.0	2.3	−6.6	68.4	20.8	14.6	−1.6
CGCM2	97.9	6.5	5.9	−0.7	70.3	19	14.9	−2.1

Table 3. Predictive skills of climatic models under GHGES B2

	Performance criterion							
	Temperature				Rainfall			
Model	R^2: %	RMSE: °C	MAE: °C	NSE	R^2: %	RMSE: mm	MAE: mm	NSE
HadCM3	94.2	3.1	2.4	−6.4	58.3	24.4	18.6	−0.9
CGCM2	97.7	6.6	5.9	−0.6	67.2	19.8	15.7	−1.9

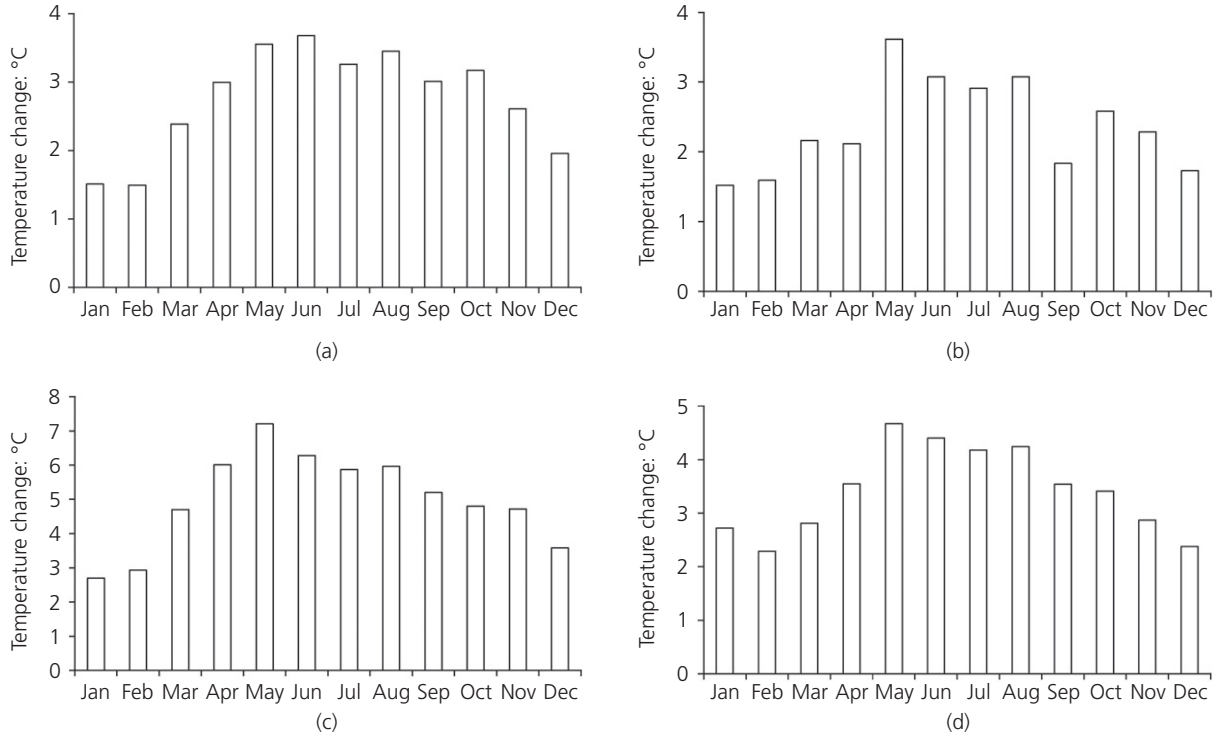

Figure 3. HadCM3 results for CCS of temperature difference in 2040–2069 under GHGES A2 (a) and GHGES B2 (b) and in 2070–2099 for GHGES A2 (c) and GHGES B2 (d)

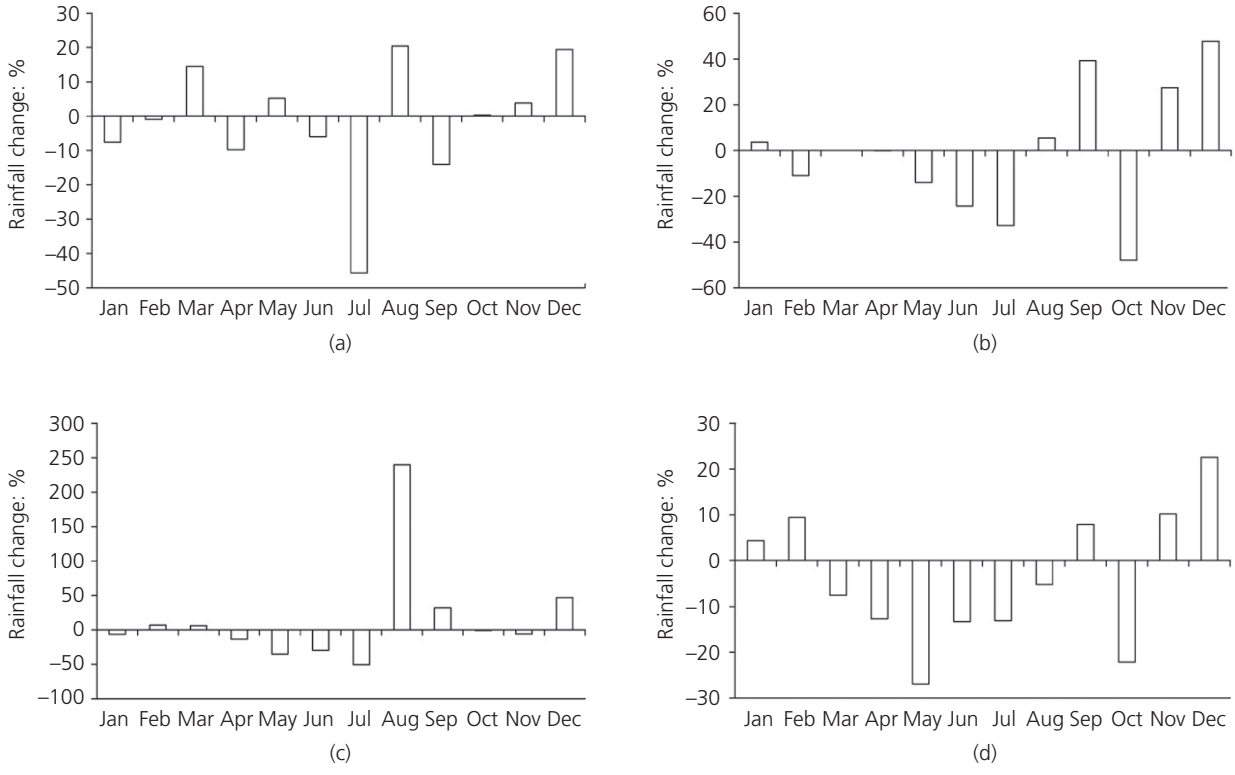

Figure 4. CGCM2 results for CCS of rainfall ratios in 2040–2069 under GHGES A2 (a) and GHGES B2 (b) and in 2070–2099 for GHGES A2 (c) and GHGES B2 (d)

−46% to 20% and −48% to 48%, respectively. For the period 2070–2099, for both GHGESs A2 and B2, the range of rainfall variation was −50% to 240% and −27% to 23%, respectively. In both scenarios and in both periods, rainfall was predicted to decrease in spring and increase in summer and autumn. Scenario B2 showed less variability than scenario A2.

Future temperature projections were calculated by adding the projected temperature differences (Figure 3) to the baseline average temperature in the corresponding season. Future rainfall projections were calculated by multiplying the projected rainfall ratios (Figure 4) by the baseline average rainfall in the period of interest (Loáiciga *et al*., 2000; Wilby and Harris, 2006).

3.2 Calibration and verification results of the IHACRES rainfall–runoff model

The IHACRES model was calibrated and validated with observed runoff. Figure 5 shows the monthly time series of calculated and observed runoff for calibration (1971–1990) and verification periods (1991–2000). The figure demonstrates the closeness of the time series of the observed runoff (LRWC, 2012) and modelled runoff in the baseline period, thus demonstrating the good predictive skill of IHACRES.

3.3 Simulation of river flow in future periods

Projected temperature from HadCM3 and projected rainfall from CGCM2 in the future periods were applied in the IHACRES model to simulate monthly time series of river flow

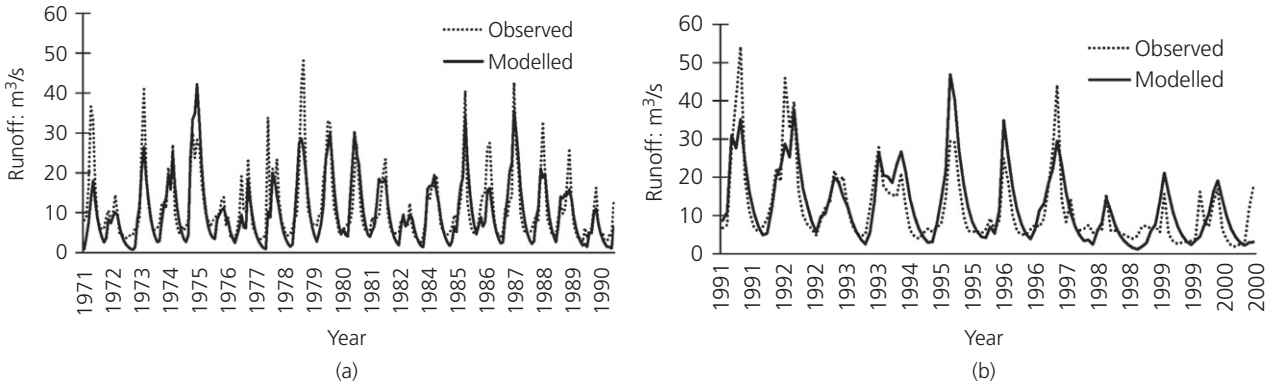

Figure 5. Comparison of monthly time series of calculated and observed runoff: (a) calibration (1971–1990) and (b) verification (1991–2000)

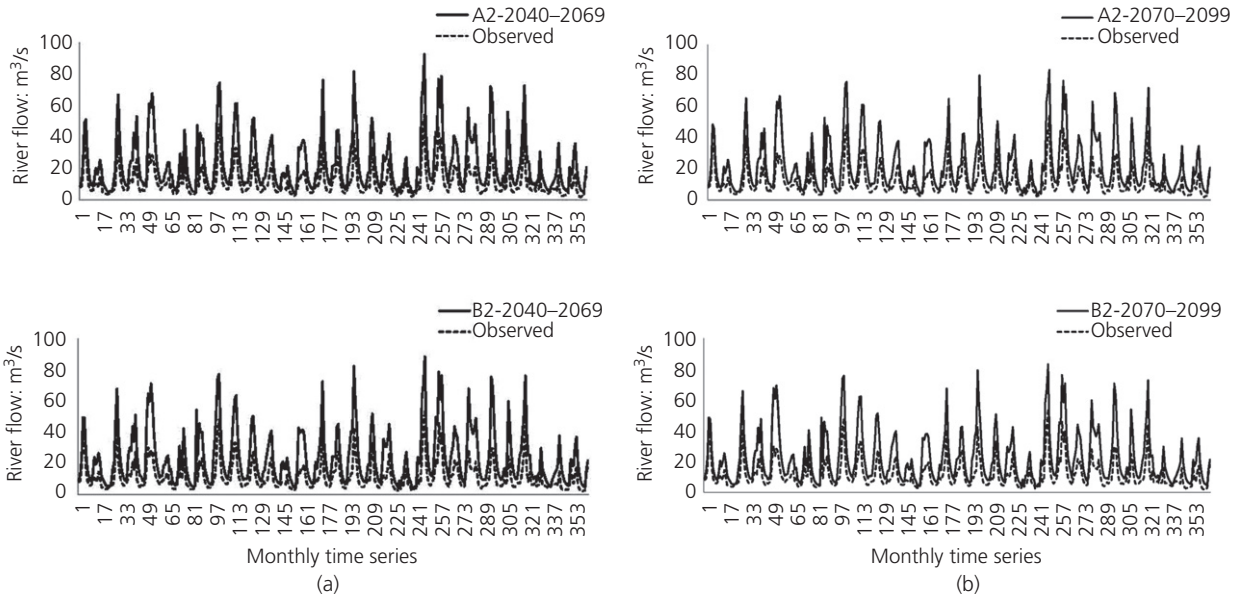

Figure 6. Comparison of monthly time series of river flow under GHGESs A2 and B2 in 2040–2069 (a) and 2070–2099 (b) with observed values

in the future periods following calibration and verification. Two thirds of the entire dataset (30 years) were used for model calibration and the remaining third was used for verification (Asadi Vaighan *et al.*, 2017; Firoozi *et al.*, 2019). Figure 6 shows the monthly river flow time series in the future periods 2040–2069 and 2070–2099 under GHGESs A2 and B2, along with the observed river flow values (LRWC, 2012). The runoff variations simulated by the IHACRES model relative to the baseline monthly average values are shown in Figure 7. The annual runoff variations relative to the observed values are listed in Table 4. It is evident from Figures 6 and 7 that in 2040–2069 and 2070–2099 and under GHGESs A2 and B2, compared with the baseline values, the monthly flow would decrease in late spring, summer and early autumn. The river flow would increase in winter. As shown in Table 4, the annual runoff under GHGES A2 in future periods 2040–2069 and 2070–2099 would decrease by 2.03% and 6.64%; under GHGES B2, it would decrease by 4.17% and 8.94%, respectively.

3.4 Simulation of groundwater resources

Groundwater modelling was conducted using GMS 7.1 software. For this purpose, several modules (including boundaries, observation wells, extraction wells, surface recharge, head on the boundaries etc.) were input into the GMS model. The simulated aquifer was the central aquifer of the Khorramabad basin. This aquifer has no lateral physical boundary (such as geologic faults, for example) and thus a general head boundary was applied on the assigned model boundary. The bottom bedrock elevations and initial ground level data were applied to the model's network of cells, assisted by kriging interpolation. The GMS model was calibrated. The modelling errors during calibration are listed in Table 5. The locations of the piezometers used in the calibration are shown in Figure 8. There are ten observation wells in the study area (LRWC, 2012), including seven wells with accurate data, which were used for calibration. Figure 8 also shows the calibration results and the groundwater levels interpolated at various points in the study area. Table 5 and Figure 8 demonstrate successful calibration of the groundwater model, with a mean residual of 0.01 m, mean absolute residual of 0.43 m and root mean squared residual of 0.57 m. Aquifer recharges in the baseline period and under the CCSs calculated with GMS are listed in Table 6. It is evident that the annual recharge was predicted to decrease under the CCSs compared with the recharge in the baseline period.

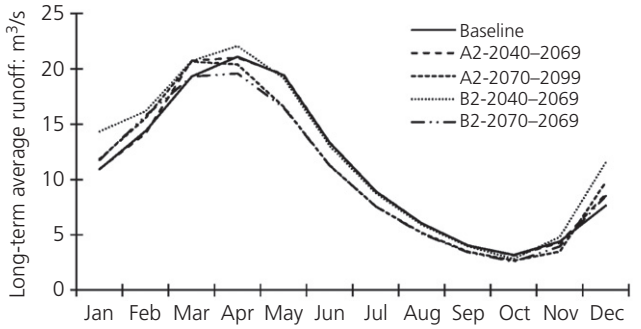

Figure 7. Long-term average monthly runoff variations relative to baseline values corresponding to combinations of emission scenarios and future periods

Table 4. Variation in annual runoff relative to observed values

Variation: %			
A2-2040–2069	A2-2070–2099	B2-2040–2069	B2-2070–2099
−2.03	−6.64	−4.17	−8.94

Table 5. ModFlow model prediction error during calibration

Type of error	Value
Mean residual	0.01 m
Mean absolute residual	0.43 m
Root mean squared residual	0.57 m
RMSE	0.5 m
Normalised RMSE	0.0004

3.5 Simulation of SWGW resources with the Weap model

Weap software was applied for simulation of water resources in the study basin. General parameters and the various components of the system (the river, groundwater, demand nodes etc.) were defined in Weap's Schematic section. Data for each component were entered in the Data section. The baseline (1971–2000) observed runoff and the runoff projections under the CCSs obtained with IHACRES were input into Weap for surface water modelling. The recharge values obtained from the GMS model in the baseline period and under CCSs were input into Weap to allocate SWGW resources. Agricultural and M&I water demands in the study region were input into Weap. Agricultural water demand in the study area is supplied with SWGW, whereas M&I water is supplied exclusively by groundwater. Figure 9 shows a summary of water resources, water demands and allocation of water resources to meet water demands.

The Weap projections considered increases in water demand in future periods of 20%, 40% and 60% greater than the baseline water demand. Future water demand can be calculated based on relative humidity, reference crop evapotranspiration, duration of solar radiation, wind speed and other pertinent variables. These data are not available in the study area for future periods. Therefore, the effect of climate change on water demand was accounted for by creating scenarios of 20%, 40% and 60% increases in agricultural and M&I water uses in the future compared with baseline conditions. These increases in water use were simulated using the Weap software. The increases of 20%, 40% and 60% were chosen based on reviews of published works dealing with projections of water use in

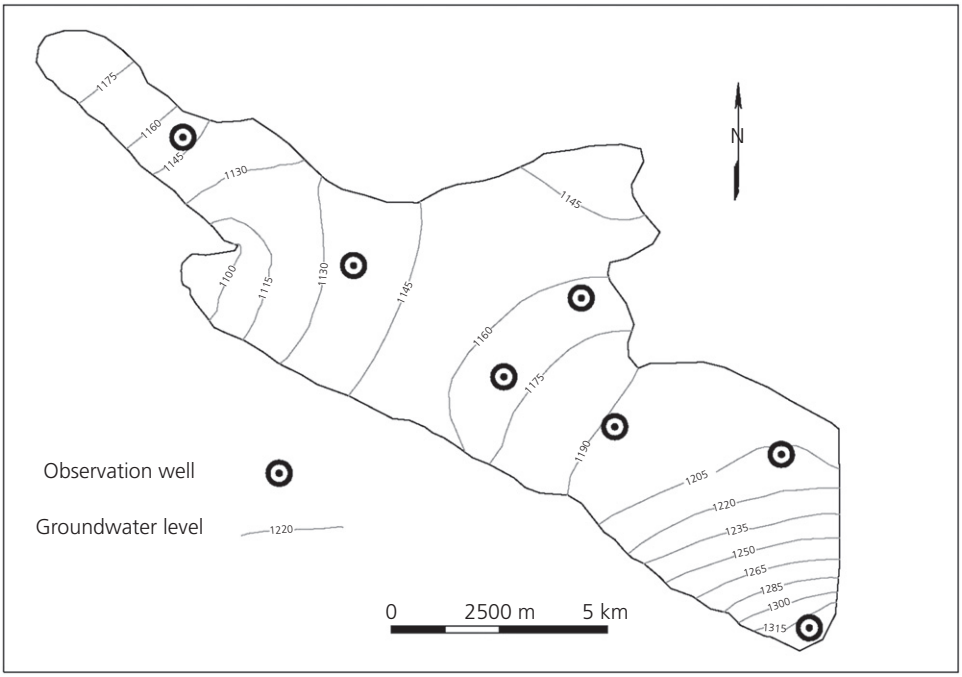

Figure 8. Location of piezometers used in calibration (the seven piezometers marked with black circles were used for calibration)

Table 6. Average annual recharge resulting from ModFlow

Average annual recharge: 10^6 m^3				
Baseline	A2-2040–2069	A2-2070–2099	B2-2040–2069	B2-2070–2099
14.0	13.8	13.2	13.6	13.0

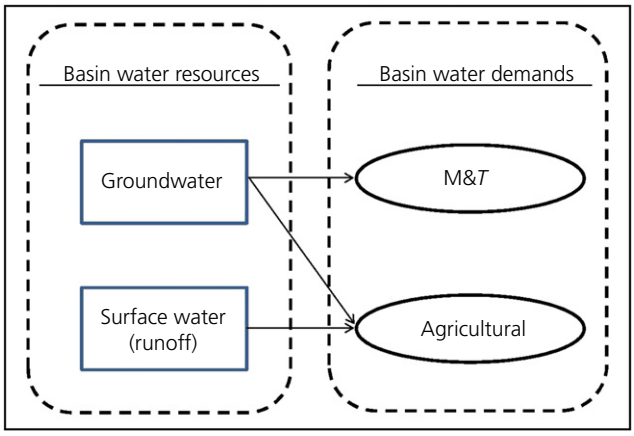

Figure 9. Diagram of water resources and water demands, the allocation of resources to water consumption

Iran. For example, Ashofteh *et al.* (2017) estimated increases in water use of 20–30%. The current authors foresee worsening conditions in the study area, and thus rises in water use of 40 and 60% were also considered. The projected water allocations were obtained for each demand node in the study region using the Weap model. The water allocation corresponding to the baseline period and the projected water allocations under the CCSs corresponding to the agricultural and M&I sectors are listed in Tables 7 and 8, respectively. As shown in these tables, increases in water allocations were projected for all CCSs relative to the baseline period for all levels of increased water demand. Specifically, for all four CCSs (A2-2040–2069, A2-2070–2099, B2-2040–2069 and B2-2070–2099) there would be larger water allocations than in the baseline period. The projected water allocations increased with an increase in water demand from 20% to 40% and then to 60%.

Unsupplied water demand (or water deficit) is defined as the difference between water demand and projected water allocation. The unsupplied average monthly water demands for the agricultural and M&I sectors in the baseline period and under the considered CCSs are listed in Tables 9 and 10, respectively.

The data in Table 10 indicate a projected water deficit in the M&I sector in autumn and summer. The deficit in the autumn

Table 7. Projected water allocation to the agricultural sector in the baseline period and under CCSs with increased water demand (relative to baseline)

	Projected water allocation: 10^6 m^3											
	Jan	Feb	Mar	Apr	May	Jun	Jul	Aug	Sep	Oct	Nov	Dec
Baseline 1971–2000	2	2	2	6	13	20	19.95	19.42	12.96	5	4.75	4.5
20% increase in water demand												
B2-2040–2069	2.38	2.38	2.38	7.16	15.51	23.79	22.94	21.88	15.44	5.96	5.67	5.37
A2-2040–2069	2.38	2.38	2.38	7.16	15.51	23.86	23.25	21.96	14.73	5.96	5.67	5.37
B2-2070–2099	2.38	2.38	2.38	7.16	15.51	23.81	22.69	21	14.42	5.96	5.67	5.37
A2-2070–2099	2.38	2.38	2.38	7.16	15.51	23.84	22.74	21.08	14.36	5.96	5.67	5.37
40% increase in water demand												
B2-2040–2069	2.77	2.77	2.77	8.32	18.02	27	24.99	22.04	17.3	6.93	6.58	6.24
A2-2040–2069	2.77	2.77	2.77	8.32	18.02	27.44	25.74	23.15	15.95	6.93	6.58	6.24
B2-2070–2099	2.77	2.77	2.77	8.32	18.02	27.07	24.71	21.97	15.25	6.93	6.58	6.24
A2-2070–2099	2.77	2.77	2.77	8.32	18.02	27.14	24.86	21.9	15.17	6.93	6.58	6.24
60% increase in water demand												
B2-2040–2069	3.16	3.16	3.16	9.48	20.54	29.53	25.5	21.61	18.08	7.9	7.5	7.11
A2-2040–2069	3.16	3.16	3.16	9.48	20.54	30.62	27.15	23.89	16.48	7.9	7.5	7.11
B2-2070–2099	3.16	3.16	3.16	9.48	20.54	29.85	25.94	21.86	15.61	7.9	7.5	7.11
A2-2070–2099	3.16	3.16	3.16	9.48	20.54	30.02	25.93	21.78	15.48	7.89	7.49	7.11

Table 8. Projected water allocation to the M&I sector in the baseline period and under CCSs with increased water demand (relative to baseline)

	Projected water allocation: 10^6 m^3											
	Jan	Feb	Mar	Apr	May	Jun	Jul	Aug	Sep	Oct	Nov	Dec
Baseline 1971–2000	4.97	4.97	4.97	6	6	6	5.79	5.65	5.30	4.83	4.83	4.83
20% increase in water demand												
B2-2040–2069	5.93	5.93	5.93	7.16	7.16	7.14	6.68	6.39	6.35	5.8	5.8	5.8
A2-2040–2069	5.93	5.93	5.93	7.16	7.16	7.16	6.78	6.41	6.05	5.8	5.8	5.8
B2-2070–2099	5.93	5.93	5.93	7.16	7.16	7.14	6.61	6.12	5.92	5.8	5.8	5.8
A2-2070–2099	5.93	5.93	5.93	7.16	7.16	7.15	6.62	6.15	5.90	5.8	5.8	5.8
40% increase in water demand												
B2-2040–2069	6.9	6.9	6.9	8.32	8.32	8.1	7.30	6.44	7.14	6.77	6.77	6.77
A2-2040–2069	6.9	6.9	6.9	8.32	8.32	8.23	7.52	6.77	6.57	6.77	6.77	6.77
B2-2070–2099	6.9	6.9	6.9	8.32	8.32	8.12	7.21	6.41	6.27	6.77	6.77	6.77
A2-2070–2099	6.9	6.9	6.9	8.32	8.32	8.14	7.26	6.39	6.24	6.77	6.77	6.77
60% increase in water demand												
B2-2040–2069	7.87	7.87	7.87	9.48	9.48	8.86	7.45	6.31	7.47	7.73	7.73	7.73
A2-2040–2069	7.87	7.87	7.87	9.48	9.48	9.19	7.95	6.99	6.79	7.73	7.73	7.73
B2-2070–2099	7.87	7.87	7.87	9.48	9.48	8.96	7.58	6.38	6.42	7.73	7.73	7.73
A2-2070–2099	7.87	7.87	7.87	9.48	9.48	9.01	7.58	6.36	6.37	7.73	7.73	7.73

is similar in the baseline period and under the CCSs. The water deficit would be more critical under the CCSs than in the baseline condition in summer, when there is higher water consumption. The water deficit is predicted to be higher in the period 2070–2099 than in 2040–2069. The water deficit in summer would be more pronounced in the agricultural sector due to higher water consumption. A comparison of the baseline period and the CCSs reveals that the four CCSs are predicted to have larger water deficits than the baseline period.

Table 11 summarises the calculated water-supply indexes (the ratio of projected water allocation to water demand) for the various periods obtained from the Weap model. The calculated water-supply indexes indicate that the water system is unable to meet 100% of the water demands under the four CCSs.

4. Concluding remarks

The effects of climate change on the conjunctive use of SWGW resources in the Khorramabad basin, Iran, were assessed in this study. Temperature projections (using the HadCM3 climate model) and rainfall projections (using the GGCM2 climate model) were calculated for two future periods (2040–2069 and 2070–2099) under GHGESs A2 and B2. The climate projections were judged to be suitable based

Table 9. Projected unsupplied water demand to the agricultural sector in the baseline period and under CCSs with increased water demand (relative to baseline)

	Unsupplied water demand: 10^6 m^3											
	Jan	Feb	Mar	Apr	May	Jun	Jul	Aug	Sep	Oct	Nov	Dec
Baseline 1971–2000	0	0	0	0	0	0	0.04	0.58	0.04	0	0	0
20% increase in water demand												
B2-2040–2069	0	0	0	0	0	0.08	0.92	1.98	0.07	0	0	0
A2-2040–2069	0	0	0	0	0	0	0.61	1.91	0.78	0	0	0
B2-2070–2099	0	0	0	0	0	0.05	1.18	2.86	1.09	0	0	0
A2-2070–2099	0	0	0	0	0	0.02	1.13	2.78	1.15	0	0	0
40% increase in water demand												
B2-2040–2069	0	0	0	0	0	0.73	2.74	5.69	0.73	0	0	0
A2-2040–2069	0	0	0	0	0	0.29	1.99	4.58	2.07	0	0	0
B2-2070–2099	0	0	0	0	0	0.66	3.02	5.76	2.78	0	0	0
A2-2070–2099	0	0	0	0	0	0.59	2.87	5.83	2.85	0	0	0
60% increase in water demand												
B2-2040–2069	0	0	0	0	0	2.07	6.09	9.99	2.45	0	0	0
A2-2040–2069	0	0	0	0	0	0.98	4.45	7.7	4.06	0	0	0
B2-2070–2099	0	0	0	0	0	1.74	5.66	9.74	4.93	0	0.01	0
A2-2070–2099	0	0	0	0	0	1.58	5.67	9.82	5.06	0	0	0

Table 10. Projected unsupplied water to the M&I sector in the baseline period and under CCSs associated with increased water demand (relative to baseline)

	Unsupplied water demand: 10^6 m^3											
	Jan	Feb	Mar	Apr	May	Jun	Jul	Aug	Sep	Oct	Nov	Dec
Baseline 1971–2000	0	0	0	0	0	0.07	0.28	0.42	0.22	0.15	0.12	0.12
20% increase in water demand												
B2-2040–2069	0	0	0	0	0	0.09	0.54	0.84	0.23	0.15	0.12	0.12
A2-2040–2069	0	0	0	0	0	0.07	0.45	0.82	0.53	0.15	0.12	0.12
B2-2070–2099	0	0	0	0	0	0.08	0.62	1.1	0.66	0.15	0.12	0.12
A2-2070–2099	0	0	0	0	0	0.07	0.6	1.08	0.68	0.15	0.12	0.12
40% increase in water demand												
B2-2040–2069	0	0	0	0	0	0.28	1.09	1.95	0.51	0.15	0.12	0.12
A2-2040–2069	0	0	0	0	0	0.15	0.86	1.62	1.08	0.15	0.12	0.12
B2-2070–2099	0	0	0	0	0	0.26	1.17	1.97	1.37	0.15	0.12	0.12
A2-2070–2099	0	0	0	0	0	0.24	1.13	1.99	4.4	0.15	0.12	0.12
60% increase in water demand												
B2-2040–2069	0	0	0	0	0	0.69	2.09	3.24	1.24	0.15	0.12	0.12
A2-2040–2069	0	0	0	0	0	0.36	1.6	2.56	1.91	0.15	0.12	0.12
B2-2070–2099	0	0	0	0	0	0.59	1.96	3.17	2.28	0.15	0.12	0.12
A2-2070–2099	0	0	0	0	0	0.54	1.96	3.19	2.34	0.15	0.12	0.12

on various performance criteria (R^2, RMSE, MAE and NSE). According to the modelling, in 2040–2069, temperature is predicted to increase (relative to baseline conditions) under scenario A2 by 1.49–3.68°C and under scenario B2 by 1.52–3.62°C; in 2070–2099, these increases were predicted to be 2.69–7.21°C and 2.29–4.67°C, respectively. Rainfall change in 2040–2069 (relative to baseline conditions) was predicted to be between −45.65% and 20.41% under scenario A2 and between −48.03% and 47.45% under scenario B2. The ranges of rainfall change in 2070–2099 (relative to baseline conditions) under scenarios A2 and B2 were predicted to be between −50.4% and 240.02% and −26.93% and 22.57%, respectively. Under scenarios A2 and B2, respectively, the IHACRES model projected long-term average annual runoff reductions (relative to baseline conditions) of 2.03% and 4.17% in 2040–2069 and 6.64% and 8.94% in 2070–2099. The GMS model predicted reductions in groundwater levels relative to baseline conditions corresponding to CCSs A2-2040–2069, A2-2070–2099, B2-2040–2069 and B2-2070–2099 of 2.3%, 3.0%, 2.5% and 3.4%, respectively. The recharge relative to the baseline conditions under these four CCSs was projected to decrease by 1.43%, 5.71%, 2.86% and 7.14%, respectively. Conjunctive water use was modelled with the Weap model for the four CCSs (A2-2040–2069, A2-2070–2099, B2-2040–2069 and B2-2070–2099) and increasing water demands of 20%, 40% and 60% relative to the baseline water demand. SWGW

Table 11. Water-supply index (ratio of projected water allocation to water demand) in the baseline period and under CCSs with increased water demand

	Water-supply index	
	M&I	Agricultural
Baseline 1971–2000	96.11	97.78
20% increase in water demand		
B2-2040–2069	91.39	93.06
A2-2040–2069	90.56	92.22
B2-2070–2099	88.06	89.72
A2-2070–2099	88.06	89.72
40% increase in water demand		
B2-2040–2069	96.11	97.78
A2-2040–2069	82.78	84.44
B2-2070–2099	80.83	82.5
A2-2070–2099	85.56	87.22
60% increase in water demand		
B2-2040–2069	96.11	97.78
A2-2040–2069	75	76.67
B2-2070–2099	75.83	77.5
A2-2070–2099	80.28	81.94

resources were then simulated under the stated conditions of demand and climate projections.

The Weap modelling predicted that M&I and agricultural water demands would not be met under these future climate conditions. Specifically, the amount of unsupplied annual water demand in the agricultural sector under CCSs A2-2040–2069, A2-2070–2099, B2-2040–2069 and B2-2070–2099 was predicted to be 3.3×10^6 m^3, 5.08×10^6 m^3, 3.05×10^6 m^3 and 5.18×10^6 m^3 for an increased water demand of 20% of the baseline water demand. For an increased water demand of 40%, these deficits were predicted to be 8.93×10^6 m^3, 12.13×10^6 m^3, 9.88×10^6 m^3 and 12.22×10^6 m^3. For an increased water demand of 60%, these values increased to 17.19×10^6 m^3, 22.13×10^6 m^3, 20.6×10^6 m^3 and 22.08×10^6 m^3, respectively.

For the M&I sector, the amount of unsupplied annual water demand under CCSs A2-2040–2069, A2-2070–2099, B2-2040–2069 and B2-2070–2099 was predicted to be 2.25×10^6 m^3, 2.83×10^6 m^3, 2.08×10^6 m^3 and 2.85×10^6 m^3), respectively, for an increased water demand of 20% relative to the baseline water demand. For increased water demands of 40% and 60%, these deficits increased to 4.09, 5.15, 4.21 and 5.17 ($\times 10^6$ m^3) and 6.81, 8.43, 7.64 and 8.39 ($\times 10^6$ m^3), respectively.

Data availability

Some or all data, models or code generated or used during the study are available in a repository or online. Some or all data, models or code generated or used during the study are also available from the corresponding author on request.

REFERENCES

Alslevavni IN and Almohseen KA (2017) Integrated application of (Modflow) and (Weap) model in Nineveh province. *Journal of Duhok University* **20(1)**: 680–690.

Asadi Vaighan A, Talebbeydokhti N and Massah Bavani A (2017) Assessing the impacts of climate and land use change on streamflow, water quality and suspended sediment in the Kor River basin, southwest of Iran. *Environmental Earth Sciences* **76(15)**, https://doi.org/10.1007/s12665-017-6880-6.

Ashofteh PS, Bozorg-Haddad O, Akbari-Alashti H and Mariño MA (2015) Determination of irrigation allocation policy under climate change by genetic programming. *Journal of Irrigation and Drainage Engineering* **141(4)**, https://doi.org/10.1061/(ASCE)IR.1943-4774.0000807.

Ashofteh PS, Rajaee T and Golfam P (2017) Assessment of water resources development projects under conditions of climate change using efficiency indexes (EIs). *Water Resources Management* **31(12)**: 3723–3744, https://doi.org/10.1007/s11269-017-1701-y.

Azadi F, Ashofteh PS and Loáiciga HA (2019) Reservoir water-quality projections under climate-change conditions. *Water Resources Management* **33(1)**: 401–421, https://doi.org/10.1007/s11269-018-2109-z.

Buras N (1963) Conjunctive operation of dams and aquifers. *Journal of the Hydraulics Division* **89(6)**: 111–131.

Dettinger MD, Cayan DR, Meyer M and Jeton AE (2004) Simulated hydrologic responses to climate variations and change in the Merced, Carson, and American River basins, Sierra Nevada, California, 1900–2099. *Climate Change* **62(1–3)**: 283–317.

Firoozi F, Roozbahani A and Massah Bavani AR (2019) Developing a framework for assessment of climate change impact on thermal stratification of dam reservoirs. *International Journal of Environmental Science and Technology* **17**: 2295–2310.

Golfam P, Ashofteh PS and Loáiciga HA (2019) Evaluation of the VIKOR and FOWA multi-criteria decision making methods for climate-change adaptation of agricultural water supply. *Water Resources Management* **33(8)**: 2867–2884, https://doi.org/10.1007/s11269-019-02274-z.

Heydari F, Saghafian B and Delavar M (2016) Coupled quantity-quality simulation-optimization model for conjunctive surface-groundwater use. *Water Resources Management* **30(12)**: 4381–4397, https://doi.org/10.1007/s11269-016-1426-3.

IPCC (Intergovernmental Panel on Climate Change) (2007) Summary for policymakers. In *Climate Change 2007: The Physical Science Basis. Contribution of Working Group I to the Fourth Assessment Report of the Intergovernmental Panel on Climate Change*. Cambridge University Press, Cambridge, UK, p. 18.

IPCC-TGCIA (Intergovernmental Panel on Climate Change, Task Group on Scenarios for Climate Impact Assessment) (1999) *Guidelines on the Use of Scenario Data for Climate Impact and Adaptation Assessment, Version 1* (Carter TR, Hulme M and Lal M (eds)). Intergovernmental Panel on Climate Change, Task Group on Scenarios for Climate Impact Assessment, pp. 69.

Jakeman AJ and Hornberger GM (1993) How much complexity is warranted in a rainfall–runoff model? *Water Resources Research* **29(8)**: 2637–2649, https://doi.org/10.1029/93WR00877.

Jones PD and Hulme M (1996) Calculating regional climatic time series for temperature and precipitation: methods and illustrations. *International Journal of Climatology* **16(4)**: 361–377, https://doi.org/10.1002/(SICI)1097-0088(199604)16:4<361::AID-JOC53>3.0.CO;2-F.

Karamouz M, Tabari MR and Kerachian R (2004) Conjunctive use of surface and groundwater resources: application of genetic algorithms and neural networks. In *Critical Transitions in Water and Environmental Resources Management* (Sehlke G, Hayes DF

and Stevens DK (eds)). ASCE, Reston, VA, USA, https://doi.org/abs/10.1061/40737%282004%2990.

Karamouz M, Tabari MR, Kerachian R and Zahraie B (2005) Conjunctive use of surface and groundwater resources with emphasis on water quality. In *Impacts of Global Climate Change* (Walton R (ed.)). ASCE, Reston, VA, USA, https://doi.org/10.1061/40792%28173%29360.

Korkmaz S, Pekkan E and Güney Y (2016) Transient analysis with MODFLOW for developing water-diversion function. *Journal of Hydrologic Engineering* **21(6)**, https://doi.org/10.1061/(ASCE)HE.1943-5584.0001349.

Lane ME, Kirshen PH and Vogel RM (1999) Indicators of impact of global climate change on U.S. water resources. *Journal of Water Resources Planning and Management* **125(4)**: 194–204, https://doi.org/10.1061/(ASCE)0733-9496(1999)125:4(194).

Li Z, Quan J, Li XY *et al.* (2016) Establishing a model of conjunctive regulation of surface water and groundwater in the arid regions. *Agricultural Water Management* **174**: 30–38, https://doi.org/10.1016/j.agwat.2016.04.030.

Loáiciga HA, Maidment D and Valdes JB (2000) Climate change impacts in a regional karst aquifer, Texas, USA. *Journal of Hydrology* **227(1–4)**: 173–194.

LRWC (Lorestan Regional Water Corporation) (2012) *Water Resources Allocation Report of Khorramabad Study Area*. LRWC, Khorramabad, Iran.

Mani A, Tsai FTC and Paudel KP (2016) Mixed integer linear fractional programming for conjunctive use of surface water and groundwater. *Water Resources Planning and Management* **142(11)**, https://doi.org/10.1061/(ASCE)WR.1943-5452.0000676.

Mitchell TD (2003) Pattern scaling: an examination of the accuracy of the technique for describing future climates. *Climatic Change* **60(3)**: 217–242.

Moghadam SH, Ashofteh PS and Loáiciga HA (2019) Application of climate projections and Monte Carlo approach for the assessment of future river flow: case study of the Khorramabad River basin, Iran. *Journal of Hydrologic Engineering* **24(7)**: 05019014, https://doi.org/10.1061/(ASCE)HE.1943-5584.0001801.

Raskin P, Hansen E, Zhu J and Iwra M (1992) Simulation of water supply and demand in the Aral Sea region. *Water International* **17(2)**: 55–67, https://doi.org/10.1080/02508069208686127.

Safavi HR and Falsafioun M (2017) Conjunctive use of surface water and groundwater resources under deficit irrigation. *Journal of Irrigation and Drainage Engineering* **143(2)**, https://doi.org/10.1061/(ASCE)IR.1943-4774.0001122.

Safavi HR, Darzi F and Mariño MA (2009) Simulation-optimization modeling of conjunctive use of surface water and groundwater. *Water Resources Management* **24**: 1965–1988.

Singh A (2014) Conjunctive use of water resources for sustainable irrigated agriculture. *Journal of Hydrology* **519**: 1688–1697.

Tabari MMR (2015) Conjunctive use management under uncertainty conditions in aquifer parameters. *Water Resources Management* **29**: 2967–2986.

Tabari MMR and Soltani J (2012) Multi-objective optimal model for conjunctive use management using SGAs and NSGA-II models. *Water Resources Management* **27**: 37–53.

Wilby RL and Harris I (2006) A framework for assessing uncertainties in climate change impacts: low flow scenarios for the River Thames, UK. *Water Resources Research* **42(2)**: 1–10.